Overview on the Progress of the Conceptual Studies of a Gamma Ray Spectrometer Instrument for DEMO

L. Giacomelli,[a,1] M. Nocente,[b] E. Perelli Cippo,[a] M. Rebai,[a] D. Rigamonti,[a] M. Tardocchi,[a] C. Cazzaniga,[c] M. Cecconello,[d] S. Conroy,[d] A. Hjalmarsson,[d] G. Ericsson,[d] T. Franke[e] and W. Biel[f]

[a] *Istituto per la Scienza e Tecnologia dei Plasmi, Consiglio Nazionale delle Ricerche, Milan, Italy*
[b] *Dipartimento di Fisica "G. Occhialini", Università degli Studi di Milano-Bicocca, Milan, Italy*
[c] *STFC, Rutherford Appleton Laboratory, Didcot, United Kingdom*
[d] *Department of Physics and Astronomy, Uppsala University, Uppsala, Sweden*
[e] *Max-Planck-Institut für Plasmaphysik and EUROfusion Power Plant Physics and Technology (PPPT) Department, Garching, Germany*
[f] *Institute of Energy- and Climate Research, Forschungszentrum Jülich GmbH, Germany and Department of Applied Physics, Ghent University, Belgium*
E-mail: Luca.Giacomelli@istp.cnr.it; Luca.GIACOMELLI@ec.europa.eu

ABSTRACT: The future DEMO tokamak will be equipped with a suite of diagnostics which will operate as sensors to monitor and control the position and operation parameters of DT plasmas. Among the suite of sensors, an integrated neutron and gamma-ray diagnostic system is also studied to verify its capability and performance in detecting possible DEMO plasma position variations and contribute to the feedback system in maintaining DEMO DT plasma in stable conditions. This work describes the progress of the conceptual study of the gamma-ray diagnostic for DEMO reactor performed during the first Work-Package contract 2015-2020.

The reaction of interest for this Gamma-Ray Spectrometer Instrument (GRSI) consists of D(T, γ)^{5}He with the emission of 16.63 MeV γ rays. Due to DEMO tokamak design constraints, the gamma and neutron diagnostics are integrated, both featuring multi-line of sight (camera type), viewing DEMO plasma radially with vertical (12) and horizontal (13) viewing lines to diagnose the γ and neutron emission from the DT plasma poloidal section.

The GRSI design is based on the investigation of the reaction cross sections, on the calculations performed with GENESIS and MCNP simulation codes and on the physics and geometry constrains of the integrated instrument. GRSI features long collimators which diameters are constrained by the neutron flux at the neutron detectors of the Radial Neutron Camera (RNC) system placed in front, which are key to control DEMO DT plasma position. For these reasons, only few GRSI parameters can be independently selected to optimize its performance. Among these, the choice of the collimator diameters at the back side of the neutron detector box up to the GRSI detector, the use of LiH neutron attenuators in front of the GRSI detectors, the GRSI detector material and shielding.

The GRSI detector is based on commercial $LaBr_3$(Ce) inorganic scintillating crystal coupled with a photomultiplier tube or a Silicon photomultiplier. They are designed to operate at high count rate although GRSI geometry constraints severely impact on this feature. The GRSI can also provide an independent assessment of DEMO DT fusion power and T burning.

KEYWORDS: DT fusion plasmas; DEMO diagnostics; high-energy gamma-ray spectroscopy; $LaBr_3$(Ce) inorganic scintillating detector.

---

[1] Corresponding author.

Contents

1. Introduction **1**

2. Progress on GRSI design to optimize its performance for DEMO plasma position control **2**

2.1 GRSI detector geometry and collimators 2

2.2 Assessment of the GRSI measured 16.63 MeV DT gamma-ray spectrum 3

2.3 Assessment of the GRSI gamma-ray and neutron cross-talk in nearby detectors 4

2.4 Assessment of the GRSI shielding material on measured gamma-rays 4

2.5 GRSI capability of measuring impurity concentration in DEMO DT plasmas 5

2.6 Effects of the DTγ/DTn branching ratio on the GRSI performance 6

2.7 GRSI capability of assessing DEMO DT fusion power with gamma-ray measurements 7

2.8 GRSI capability of assessing the nT/nD ratio 9

3. Discussion **10**

1. Introduction

The design of the diagnostics for the position control of DEMO Deuterium-Tritium (DT) plasmas completed its first six-year long design contract and underwent an external panel review [1][2][3]. The Gamma-Ray Spectrometer Instrument (GRSI) is one of these set of diagnostics. It aims at the spectroscopic measurements of DT gamma-ray emission of $D(T,\gamma)^5He$ and $T(p,\gamma)^4He$ reactions of 16.63 MeV (DTγ) and 19.81 MeV (Tpγ), respectively, to be able to monitor and control the DT plasma position during the DEMO discharge with 10 ms time resolution [2][3].

The GRSI is thought to be installed at the back side of the Neutron Vertical and Horizontal Cameras (VNC and HNC, respectively) [4], outside DEMO biological shielding with very long collimators. With respect to the initial studies [5], new aspects of the GRSI design have been considered [6], namely:

1) the count rate sensitivity to detector and collimator geometry;
2) the GRSI capability and accuracy for DEMO plasma position control;
3) DTγ and DTn cross-talk in nearby GRSI detectors;
4) effects of the shielding materials on GRSI performance;
5) capability in assessing the impurity concentrations in DEMO DT plasmas by measuring their X-ray emission;
6) effects of the accurate knowledge of DTγ/DTn branching ratio (BR) on the GRSI performance;
7) capability of assessing DEMO DT fusion power via γ ray measurements;
8) capability of assessing the density nT/nD ratio.

All these aspects are reported and discussed in the following section which provide an overview on the status of the project and on the choices for the further development of the GRSI design.

2. Progress on GRSI design to optimize its performance for DEMO plasma position control

2.1 GRSI detector geometry and collimators

The Radial Neutron Camera (RNC) is designed with fan-shaped collimators, 12 for the Vertical Neutron Camera (VNC) and 13 for the Horizontal Neutron Camera (HNC). Each RNC collimator is designed as a very long cylinder in front of the RNC neutron detector box which sees directly DEMO vessel and its incoming neutron flux. The GRSI is planned to be installed at the backside of the RNC making use of the same lines of sight. The GRSI collimators are defined as a cylinder from the backside of the RNC neutron detector box to the front of GRSI detector. This design constraint has been investigated in terms of GRSI detector and collimator diameters in order for the GRSI to reach count rates compatible with the diagnosis and control of DEMO plasma position. Two geometries of DTγ spectrometers based on $LaBr_3$(Ce) inorganic scintillating material [7] have been considered to assess their efficiency: commercial 7.62 cm x 15.24 cm (3"x6" diameter x length) and 9.65 cm x 24.64 cm (3.8"x9.7"). A Monte Carlo model based on MCNP code [8] has been setup to evaluate their detection efficiency for incoming DTγ flux of 16.63 MeV: These result in 93 % and 99 %, respectively. The RNC neutron fluxes at the various neutron detector positions have been used as input to assess the corresponding γ count rate based on the assessment of BR in literature and on GRSI geometry. At the beginning of the GRSI design in 2015, the BR was studied considering the available literature reporting of experimental assessments performed in 1980s and 1990s for various centre of mass DT energies. Each assessment features its own experimental uncertainties. To find the BR value correspondent to DEMO burning plasma conditions, a fit of all these BR values has been performed and a conservative extrapolated BR value of $2.07 \cdot 10^{-6}$ obtained [5].

The simulation code GENESIS [9] has been used to define the input 14.01 MeV DT neutron (DTn) spectrum for DEMO DT plasmas at equilibrium temperatures of 10 keV, 20 keV and 50 keV. The DTγ spectrum has been then obtained considering the DTn cross section and the DTγ/DTn branching ratio BR = $2.07 \cdot 10^{-6}$ [5], while the Tpγ spectrum directly from Tp cross sections [6].

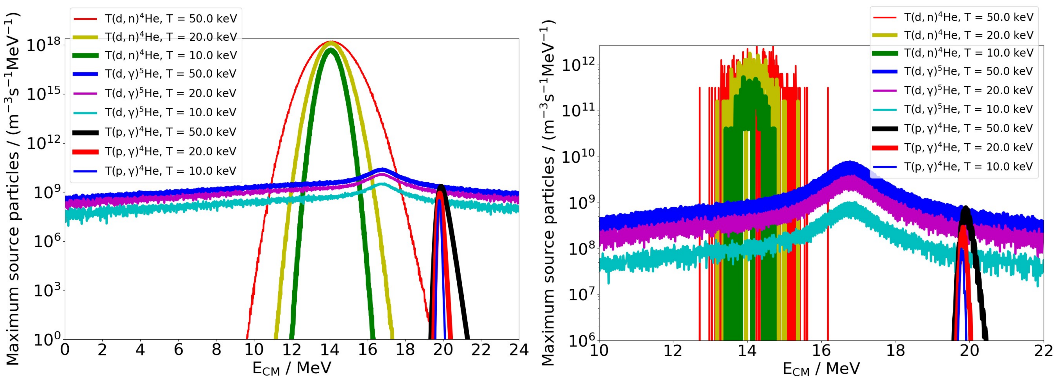

Figure 1. On the left panel, incoming DTn, DTγ and Tpγ spectra distributions for DEMO thermal plasmas at 10 keV, 20 keV and 50 keV. On the right panel, the corresponding spectra at the GRSI detector position after travelling through 120.0 cm long LiH neutron attenuator.

A key component of the GRSI consists of a LiH neutron attenuator positioned in front of the GRSI detectors to suppress the incoming DTn flux. Based on MCNP calculation, 120.0 cm long

LiH cylinder featuring attenuation factors of 10^6 to DTn and 0.3 to DTγ has been found suited for the GRSI designed. Figure 1 shows the effects of LiH neutron attenuator for DT plasmas at different equilibrium temperatures.

The impact of the RNC and GRSI collimator diameters on the DTγ GRSI measurement have been evaluated in terms of DTγ count rates. Different diameters of the GRSI collimators, namely, 1.10 cm, 2.20 cm, 4.20 cm and 6.62 cm, have been studied to assess the GRSI count rate capability. In Table 1 the maximum count rates at the GRSI central channel detector of the vertical and horizontal arrays are reported for detector dimensions of 3"x6" and 3.8"x9.7". With 6.62 cm diameter collimators, GRSI would reach 2.5 times higher count rates of pure DTγ events with respect to 4.20 cm. The edge channels features about half the rate of the central channels as displayed in Figure 2.

Table 1. Maximum count rates (in kCounts/s) assessed for the vertical and horizontal GRSI central channel for collimator diameters of 2.20 cm, 4.20 cm and 6.62 cm and detector dimensions of 3"x6" and 3.8"x9.7".

GRSI detector	GRSI V 2.20 cm	GRSI H 2.20 cm	GRSI V 4.20 cm	GRSI H 4.20 cm	GRSI V 6.62 cm	GRSI H 6.62 cm
3"x6"	0.32	0.21	1.28	0.83	3.32	2.12
3.8"x9.7"	0.34	0.22	1.37	0.89	3.55	2.27

Now, considering the effects of the background (the larger the detector volume the larger its sensitivity to the 4π distributed neutron and γ background), the commercial costs and the instrument performance, the GRSI for DEMO can implement 3"x6" $LaBr_3$(Ce) scintillators similarly to the ones already installed and operational at the Joint European Torus (JET, Culham, UK) [10] and those defined for the Radial Gamma-Ray Spectrometers (RGRS) system for ITER [11].

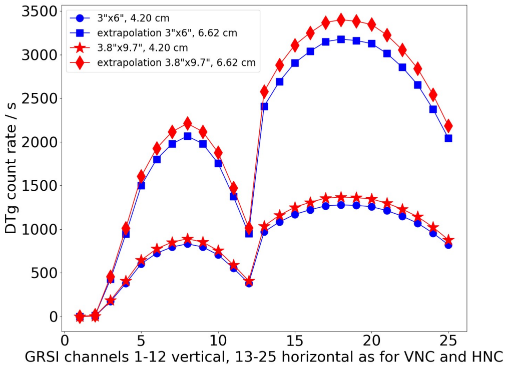

Figure 2. Comparison of the GRSI DTγ count rates measured in each vertical (1-12) and horizontal (13-25) channel for 4.20 and 6.62 cm diameters and for 3"x6" and 3.8"x9.7" $LaBr_3$(Ce) scintillators.

2.2 Assessment of the GRSI measured 16.63 MeV DT gamma-ray spectrum

The effects of the DTn induced background on the direct DTγ spectrum has been investigated assuming GRSI 4.20 cm diameter collimators equipped with 120.0 cm long LiH neutron attenuators in front of the 3"x6" $LaBr_3$(Ce) scintillators. Figure 3 displays the simulated GRSI measured γ spectrum. About 93.5 % of the total events in the spectrum fall below 10 MeV of which 99.9 % are due to DTn induced background events. 98.6 % of 16.63 MeV DTγ events are above 10 MeV with the 19.81 MeV Tpγ spectrum depressed by a factor 200. These results confirm GRSI DTγ detection as mostly background-free.

Given the characteristic and quality of the GRSI measurements, a 3"x6" $LaBr_3(Ce)$ scintillator may be capable of 80 genuine DTγ counts per 100 ms for DEMO position control. This does not match DEMO requirements on time resolution (10 ms) and accuracy but, given the GRSI installation constraints and their impact on its performance, the GRSI can still be used to benchmark the RNC diagnostic measurements and to provide physics information on more relaxed time resolutions.

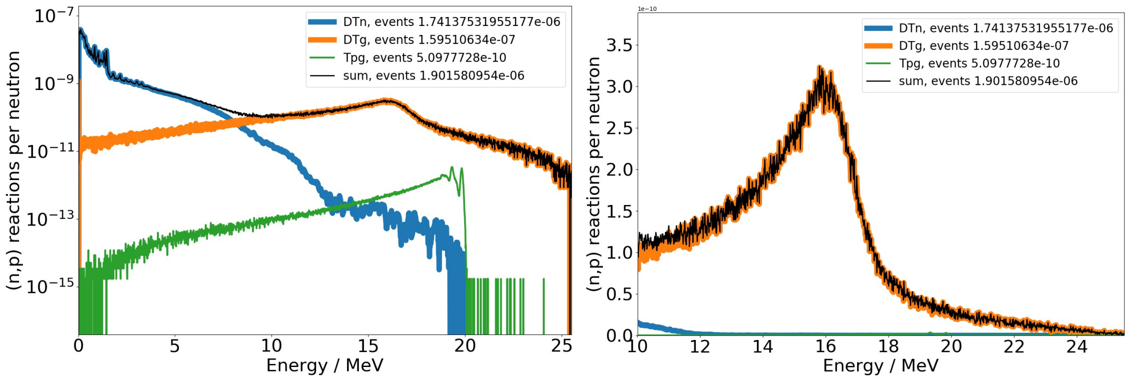

Figure 3. On the left panel, comparison of DTn, DTγ and Tpγ contribution to the simulated GRSI measured gamma-ray spectrum in log scale. On the right panel, the same in linear scale (times $1{\cdot}10^{-10}$) for deposited energies in $LaBr_3(Ce)$ scintillator larger than 10 MeV.

2.3 Assessment of the GRSI gamma-ray and neutron cross-talk in nearby detectors

Being the GRSI, as the RNC, a multi-line of sight instrument, the cross-talk of neighboring channels needs to be taken into account. The scattered events in one GRSI channel/detector into the neighboring one hampers the accuracy of the plasma position information available from the measurement of each individual channel/detector and on the DTγ profile reconstruction as a whole. MCNP calculations have been carried out for incoming DTγ and DTn along one specific line of sight (4.20 cm diameter) into its 3"x6" scintillator to assess the number of events detected also in the nearby similar detector. The shielding is assumed to be made of B_4C as in the RNC design [4]: Natural Boron is considered with density of 2.5 g/cm^3 and approximately 20% of ^{10}B and 80% of ^{11}B. The cross-talk induced by DTγ results in an exponentially distributed energy spectrum up to 6 MeV and a factor $5.22{\cdot}10^{-2}$ lower with respect to the direct spectrum. The cross-talk induced by neutrons is thus negligible [6].

2.4 Assessment of the GRSI shielding material on measured gamma-rays

Three different materials (B_4C, barite concrete and EUROFER) have been investigated for the GRSI shielding modeled in MCNP [8] and considering the simulated measurement of direct DTγ, induced cross-talk and background events. As shown in Figure 4 on the left, the B_4C shielding (black line) seems to feature a larger number of simulated events within 5-15 MeV range for fluxes lower than 15 MeV/cm^2 in the direct measured spectrum and larger than 3 MeV/cm^2 in the cross-talk spectrum (on the right). Now the impact of the background caused by the shielding material can be quantified considering the number of good events above 10 MeV in the spectra. Figure 5 illustrates the fractions of direct and background events below and above 10 MeV energy threshold depending on the shielding material. Barite concrete shielding features the largest fraction of good events above 10 MeV, 5.4 % better than B_4C, and the lowest background.

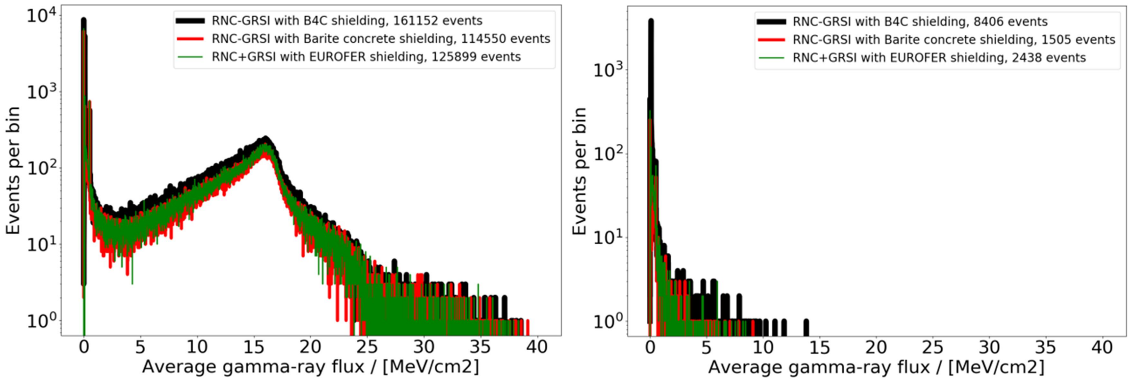

Figure 4. Comparison of the direct (left) and cross-talk (right) DTγ simulated spectra measured along two neighbouring lines of sight of the GRSI shielded with B_4C, barite concrete or EUROFER.

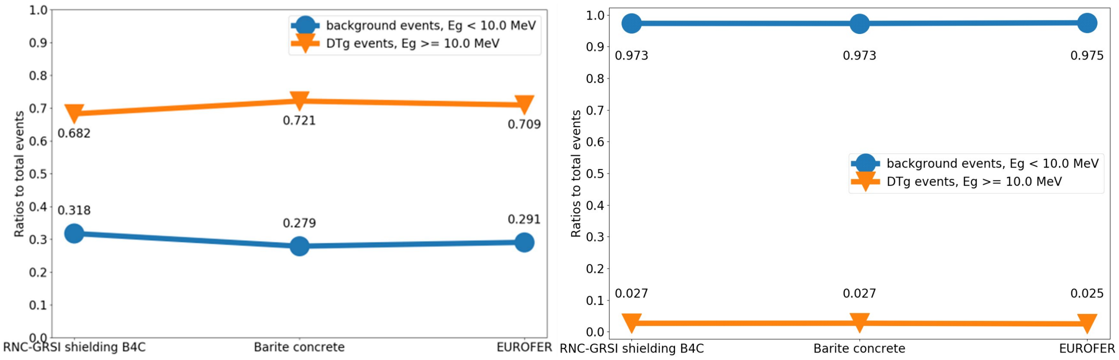

Figure 5. Comparison of the fractions of good events and background in the direct (left) and cross-talk (right) DTγ simulated spectrum measured along two neighbouring lines of sight of the GRSI shielded with B_4C, barite concrete or EUROFER.

2.5 GRSI capability of measuring impurity concentration in DEMO DT plasmas

DEMO DT plasmas will feature impurities of W, Xe, Kr, Ar, Fe, all at very low concentrations. The cross-sections and energies of their X-ray emission has been studied in order to verify the GRSI capability of detecting it. These impurities emit several low energy (about 10^2 keV) X rays from nuclear excited states with reactions cross sections of about 1 barn (10^{-28} m^2). In case of Tungsten, the typical plasma electron density is about 10^{20} electrons/m^3 with Tungsten concentration ratios in the tokamak vessel of $n_W/n_e = 10^{-4}$. In these conditions, the low Tungsten concentration ($n_W = 10^{16}$ W atoms/m^3) and X-ray energy emissions (about 10^2 keV) result in X-rays which may be detected in the region of $LaBr_3$(Ce) intrinsic activity (up to 3 MeV, see Figure 11) and not clearly recognizable [7]. This is also true for the other impurities investigated.
In fact the detector crystal for the GRSI project made of $LaBr_3$(Ce) has been optimized for the diagnosis of 16.63 MeV DT γ rays. If the goal of the measurement would be the diagnosis of the X-ray emission of plasma impurities, a dedicated diagnostic with different geometry constraints and detector material and/or technology (i.e., gas electron multiplier GEM detectors) would have to be considered.
Also the diagnosis of fusion reactions involving ^{3}He has been considered in the GRSI assessment. ^{3}He spatial distribution, accumulation, "thermal" and "high energy" fraction with few seconds time resolution are of interest to assess the DT burning efficiency: In DT plasmas at a certain temperature, ^{3}He is produced from DD reactions with 50 % branching ratio and two orders of magnitude lower cross section than DT. In its slowing down motion and ion/electron

collisions in DT plasmas, ^3He may react with D giving rise to ^5Li and 16.60 MeV γ rays (10^{-3} branching ratio). As this reaction results from a low probability two-step process with energy similar to the direct DTγ of interest, the ^3He signature is difficult to be diagnosed with the GRSI.

2.6 Effects of the DTγ/DTn branching ratio on the GRSI performance

The DTγ/DTn branching ratio BR = $2.07 \cdot 10^{-6}$ used for the GRSI design has been initially extrapolated from literature [5], as mentioned in Section 2.1. More recent observations and measurements of DTγ at OMEGA and NIF [12] provided an accurate estimate of BR equal to $4.20 \cdot 10^{-5}$, 20 time larger than the previous conservative assumption of $2.07 \cdot 10^{-6}$ with a big impact on the GRSI overall performance (Figure 6) [5][6].

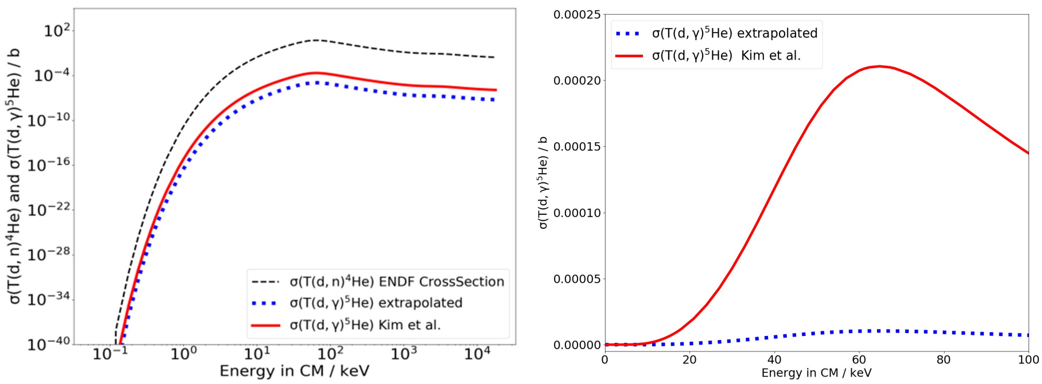

Figure 6. Comparison of the DTn cross section (black dashed line) with the derived DTγ cross sections obtained for BR values of $2.07 \cdot 10^{-6}$ (blue dotted line) and of $4.20 \cdot 10^{-5}$ (red line).

With this new BR value, the evaluation of the GRSI performance for DEMO plasma position control have been reassessed for different RNC geometry, i.e., collimator diameters, configurations [4]: Figure 7 shows GRSI DTγ count rates above 10 MeV in range of 0.01-7.50 kCounts/s for 7.0 cm diameter collimator. If 9.0 cm diameter collimator is considered, the count rates result about 30-40 % larger.

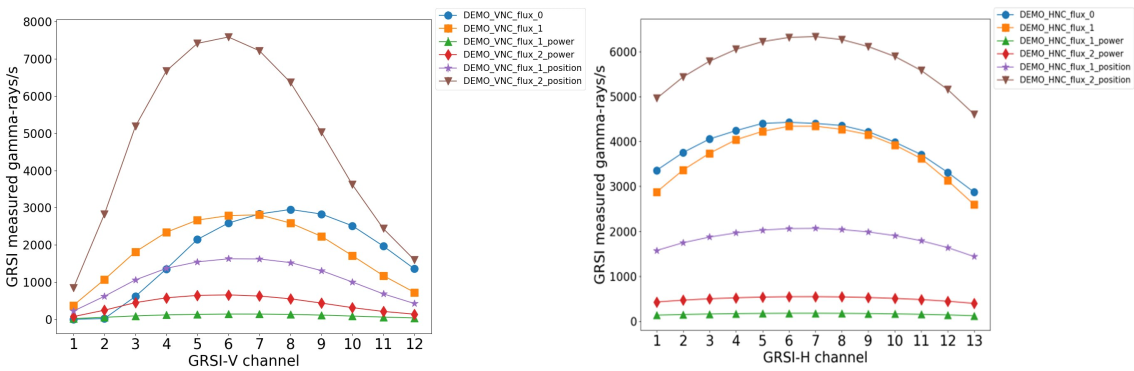

Figure 7. Comparison of GRSI simulated DTγ rates (vertical channels 1-12 on the left; horizontal channels 1-13 on the right) of energy events above 10 MeV for different RNC configurations: flux 0 and 1; flux 0 and 1 power; flux 0 and 1 energy [4]. Input parameters BR = $4.20 \cdot 10^{-5}$, 7.0 cm diameter collimator, 120.0 cm long LiH neutron attenuators and 3"x6" $LaBr_3(Ce)$ scintillator are assumed.

The GRSI as the RNC, being a multi-line of sight instrument with about 20 cm space resolution, can make use of the correlation of the individual measurements along each channel/detector to verify the possibility of control of DEMO plasma positioning. Considering RNC collimator geometry and the neutron fluxes [13], an asymmetry parameter [3] can be defined as

$$Asymmetry = \frac{\sum_{i=1}^{n/2} N' - \sum_{i=\frac{n}{2}+1}^{n} N'}{\sum_{i=1}^{n} N'}$$ with *N'* the measured number of counts within 10 ms (neutron for the HNC or VNC and γ rays for the GRSI) and *n* the number of lines of sight (12 for the vertical cameras VNC and GRSI, and 13 for the horizontal HNC and GRSI). The Asymmetry has been studied for both RNC and GRSI for DEMO plasma displacements in the range [-20, +20] cm with 1 cm step vertically and horizontally. A linear relationship has been assumed for the measured counts as function of the displacements such that for a vertical displacement of -20 cm towards the bottom of the vessel, the top channel of the horizontal cameras would measure 0 counts, the second from the top would measure the same counts as for the top one for 0 cm displacement, and the last detector at the bottom would measure the same counts as the previous detector with 0 cm displacement. The linearity allows to consider the fraction of counts each detector measures as the ratio of the displacement with respect to the full displacement of +20 cm or -20 cm. Moreover, the effects of displacements are independent on the two cameras such that a vertical displacement impacts only on the horizontal cameras and not on the vertical cameras although DEMO plasma is closer to or farer from it. The GRSI Asymmetry green and black trends in Figure 8 for 4.20 cm diameter collimators illustrate how the GRSI performance strongly depends on BR and how the results look similar (green) to the ones of RNC (red) when adopting BR = $4.20 \cdot 10^{-5}$ [12]. The GRSI Asymmetry trend for the conservative extrapolated BR = $2.07 \cdot 10^{-6}$ (black) improves and becomes more similar to the green trend of Figure 8 if larger GRSI collimators are implemented, for instance, already with 6.20 cm diameter.

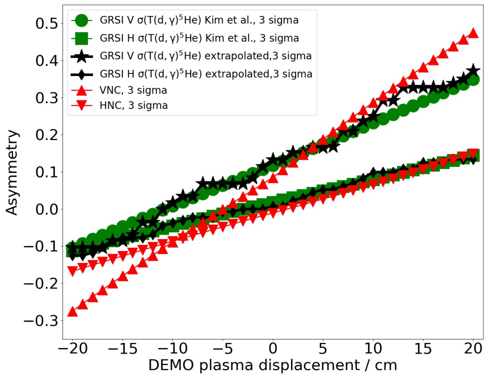

Figure 8. Comparison of the GRSI capability of detecting position variations with 1 cm spatial resolution of DEMO plasmas for BR = $4.20 \cdot 10^{-5}$ (circle and square green markers for vertical and horizontal GRSI) with respect to the extrapolated BR = $2.07 \cdot 10^{-6}$ previously used for the GRSI design (star and diamond black markers for vertical and horizontal GRSI). Both results are obtained for GRSI detector collimator of 4.20 cm diameter and compared with RNC Asymmetry trend (up and down triangle red markers for VNC and HNC).

As from the GRSI results displayed in Figure 8, although the 20 cm space resolution of the RNC-GRSI instrument, provided GRSI reaches reasonable count rates within 10 ms, which depends on RNC and GRSI collimator diameters, the Asymmetry parameter allows the GRSI (as well as the RNC) for the diagnosis of DEMO DT plasmas displacements as low as 1 cm, namely, making GRSI also theoretically capable of monitoring DEMO DT plasmas with 1 cm space resolution with 10 ms time resolution.

2.7 GRSI capability of assessing DEMO DT fusion power with gamma-ray measurements

DTγ diagnosis constitutes an independent method with respect to DTn to assess DEMO DT nuclear fusion power and, as previously noted, it is almost background-free. Another way to assess the fusion power from γ emission is to implement in DEMO the same method in use in nuclear fission reactors, namely, neutron activation of cooling water. In this case, the neutron activation reaction of interest is $^{16}O(n,p)^{16}N$ which features a Q value of 10.42 MeV. As formed, ^{16}N β^- decays with 100% branching ratio to either ^{16}O ground state or to one of its excited levels. In the latter case, γ emission to ^{16}O ground state happens with half-life of 7.14 s. Depending on the ^{16}O excited level, γ rays of 6.13 MeV (67% branching ratio) or 7.12 MeV (5%) are emitted [14]. The cross section of $^{16}O(n,p)^{16}N$ reaction is peaked about 11.65 MeV where it measures 0.115 b. For the energy of interest, namely DTn 14.05 MeV, the cross section is 0.043 b which is 37.4 % lower than the peak value [15][16][17][18].

The investigation has been carried out with MCNP calculations of DEMO divertor [6][8][19][20][21]. As presented in Figure 3 (Section 2.2), DTn induced background in $LaBr_3(Ce)$ γ spectrometer would make this γ emission hardly detectable if the spectrometer would be installed inside DEMO biological shielding. For this reason, the effect of water flow (10 m/s) and decay time (7.14 s half-life) are included in the assessment of the γ rays detectable outside the biological shielding of DEMO together with the selection of the best spectrometer for this task. The MCNP calculations have helped assess the (n,p) activation rates induced by DTn in DEMO cooling water: Oxygen isotopes ^{16}O (99.762 %), ^{17}O (0.038 %) and ^{18}O (0.2 %) are considered in the water composition. Figure 9 presents the (n,p) reaction production per neutron energy relative to the average of DTn fluence passing through the divertor (stainless steel block with a 2.035 cm layer of Tungsten facing the plasma) and reaching a 40.0 cm long and 6.41 cm radius water pipe made of EUROFER located underneath.

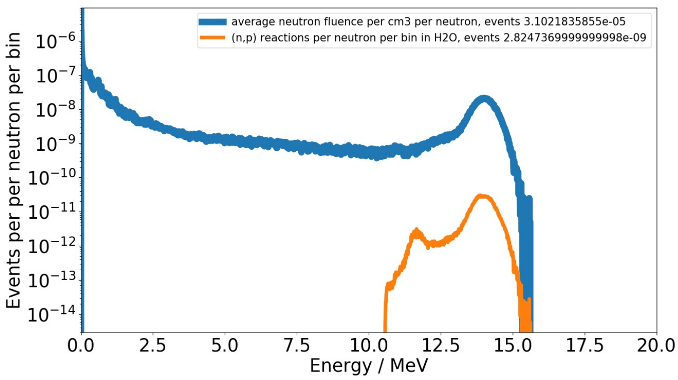

Figure 9. Comparison of the average 14 MeV DTn flux through the water pipe (thick blue line) and the (n,p) reaction production per neutron energy (thin orange line) in log scale.

The (n,p) reaction production per neutron energy for the different isotopes of Oxygen in water is compared in Figure 10 according to their molecular abundance: ^{18}O has no reaction channel (n,p). As mentioned above, $^{16}O(n,p)$ reactions in water result in ^{16}N which decays with a half-life of 7.14 s emitting γ rays of 6.13 MeV (67 % branching ratio) and of 7.12 MeV (5 %) .

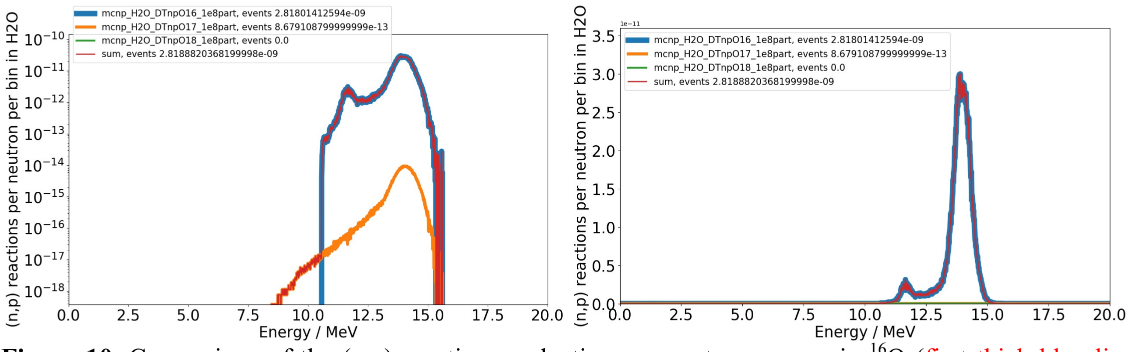

Figure 10. Comparison of the (n,p) reaction production per neutron energy in ^{16}O (first thick blue line from the top), ^{17}O (second orange line) and ^{18}O (none, third thin green line) and their sum (fourth thin red line) in log (left) and linear (right, times $1 \cdot 10^{-11}$) scales.

To assess the ^{16}N production in the water cooling pipe, different DEMO power fluxes are considered [6][22]. As an example, DEMO 1.12 W/m^2 corresponds to $4.99 \cdot 10^{13}$ 14 MeV neutrons per second per cm^2 which, according to MCNP calculations, give rise to $1.41 \cdot 10^5$ $^{16}O(n,p)^{16}N$ reactions per second per cm with the production of $9.42 \cdot 10^4$ 6.13 MeV (67 %) and of $6.89 \cdot 10^3$ 7.12 MeV (5 %) γ rays per cm. If now a 50 m long pipeline is considered to reach the measurement position outside DEMO biological shielding, the measurement can happen with a delay of 20.75 s which gives rise to $1.26 \cdot 10^4$ 6.13 MeV and to $9.19 \cdot 10^2$ 7.12 MeV γ rays per second per cm. Just for comparison to this γ emission distributed in 4π, a commercial γ source used as reference in laboratories usually features 37 kBq (37×10^3 decays per second). This confirms the possibility to design a specific γ detection system still based on $LaBr_3$(Ce) detector technology to be installed outside DEMO biological shielding and capable to assess DTn fusion power produced in DEMO similarly to what in use in nuclear fission reactors.

2.8 GRSI capability of assessing the nT/nD ratio

As presented in Figure 3 (Section 2.2), GRSI measured spectrum above 10 MeV is only relative to DTγ reactions in DEMO DT plasmas. Each DTγ measured above 10 MeV corresponds to a triton burnt in the DT nuclear fusion process. Thus, with an accurate knowledge of DTγ/DTn BR, absolute calibrated GRSI γ spectrometers and detailed modelling and calculations of the DTn induced γ background in the measured DTγ spectrum, the clear signature DTγ events above 10 MeV can be used to determine the amount of burnt T ions and contribute to the assessment of the nT/nD ratio for DEMO [23][24].
As a demonstration of the feasibility of high-energy DTγ measurements with commercial $LaBr_3$(Ce) scintillator, it is worth to mention the experience matured at JET where two high rate γ $LaBr_3$(Ce) spectrometers (3"x6") are installed with vertical-radial and equatorial-tangential lines of sight. Recently, pure T plasma experiments have been carried out. Figure 11 shows the 19.81 MeV Tpγ spectra the spectrometer with equatorial-tangential viewing line measured at JET.

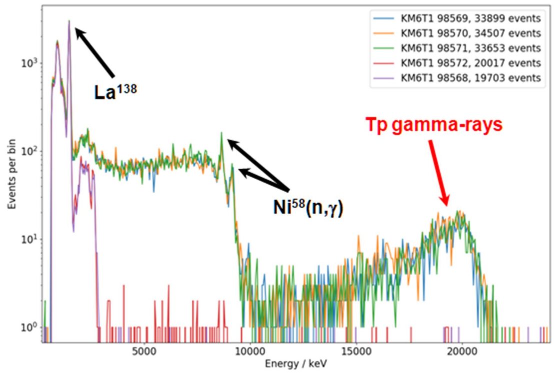

Figure 11. Comparison in log scale of measured Tpγ by a 3"x6" $LaBr_3$(Ce) spectrometer at JET during the C39 TT experimental campaign on 12th December 2020 with 96 % T, 4 % H and 4 MW Ion Cyclotron Resonance Heating. The ^{138}La and ^{58}Ni peaks are used as references for calibrating the energy scale of the measured energy spectrum. The $LaBr_3$(Ce) crystal features an intrinsic background radiation up to 3000 keV corresponding here to the spectra measured for shots 98572 and 98568 for which Tpγ emission was null.

This result confirms the MCNP calculations and modelling of the reactions of interest in GRSI design and looks very promising for DTγ spectroscopy of DT fusion plasmas with commercial $LaBr_3$(Ce) spectrometers both at ITER and for DEMO [11][5].

3. Discussion

In general, a diagnostic instrument benefits from direct viewing of the radiation source. In case of GRSI, it suffers not only from the constraints related to the RNC collimator geometry but also from the shielding effects of the RNC neutron detectors positioned along the GRSI lines of sight. Careful analysis needs to be performed to assess the impact on the DTγ fluxes when the geometry and materials of the RNC neutron detectors will be finalized. However, this study has demonstrated the capability of GRSI to control and monitor DEMO plasma positions with the combination of count rates measured along all GRSI lines of sight by the Asymmetry parameter, as for the RNC. The Asymmetry analysis makes GRSI theoretically capable of monitoring DEMO DT plasmas with 1 cm space resolution with 10 ms time resolution, provided GRSI reaches reasonable count rates within 10 ms, which mostly depends on RNC and GRSI collimator diameters.

The DTn induced γ background is in principle 4π distributed and affects the full volume of the GRSI spectrometer crystal. To reduce its impact on the DTγ measurements, the diameter of the GRSI collimators, filled with LiH neutron attenuators, at the back of the HNC-VNC neutron detector boxes should be preferably wider than the GRSI detector diameter: To maximize the detector signal-to-background ratio is best to expose its full volume to the direct incoming radiation. For these reasons as well as for possible constraints induced by the HNC-VNC geometry configurations, GRSI collimators and LiH diameters of 9.0 cm, wider than the 3" (7.62 cm) diameter of the GRSI crystal, should be considered. More detailed MCNP calculations will be required when the RNC-GRSI shielding material will be chosen. However, given the surface-to-volume ratio of DEMO DT plasmas and the GRSI geometry, the GRSI can provide equivalent diagnostic information with only 7 vertical and horizontal lines of sight with respect to the 12 and 13 of VNC and HNC.

Concerning GRSI capability of diagnosis of DT plasma impurities and assessing their concentration via X-ray emission spectroscopy, a specific instrument is recommended as well as for specific DT power measurements. Here, as performed in nuclear fission reactors, DEMO can be equipped with a GRSI similar 3"x6" $LaBr_3$(Ce) scintillator installed along the cooling water pipeline outside DEMO biological shielding.

The progress on the GRSI conceptual studies presented in this article shows the relevant potential of this diagnostic to contribute to DEMO plasma positioning control with time resolutions which depend on the RNC and GRSI collimator diameters and on the BR value. The GRSI can back up the RNC diagnostic information but being also capable of assessing independently both DEMO DT fusion power and T burning fraction from its almost background-free DTγ measurements above 10 MeV. Moreover, being so remotely installed and protected by the LiH neutron attenuators, the GRSI should not suffer the intense and prolonged DTn fluxes which impact on the materials structure. The LiH neutron attenuators will suppress the neutron direct radiation complying with the dose limits defined for DEMO outside its biological shielding.

The GRSI conceptual studies will soon enter a new phase of the DEMO diagnostics (sensors) definition, with efforts devoted to the engineering of the instrument.

Acknowledgments

This work has been carried out within the framework of the EUROfusion Consortium and has received funding from the Euratom research and training programme 2014-2018 and 2019-2020 under grant agreement No 633053. The views and opinions expressed herein do not necessarily reflect those of the European Commission.

References

[1] G. Federici et al., *DEMO design activity in Europe: Progress and updates*, Fus. Eng. Des., vol. 136, pp. 729-741 (2018) (online) https://doi.org/10.1016/j.fusengdes.2018.04.001.

[2] W. Biel et al., *DEMO diagnostics and burn control*, Fus. Eng. Des., vol. 96-97, pp. 8-15 (2015) (online) https://doi.org/10.1016/j.fusengdes.2015.01.046.

[3] W. Biel et al., *Development of a concept for the DEMO diagnostic and control system*, contribution to International Conference on DIAGNOSTICS FOR FUSION REACTORS, ICFRD 2021, Villa Monastero, September 6-10 2021, Varenna, Italy.

[4] M. Cecconello et al., *DEMO diagnostic R&D: neutron/gamma diagnostics*, (VR) Final Report on Deliverable DC-4-T004-D001, Report IDM reference No. EFDA_D_2N4SNE.

[5] L. Giacomelli et al., *Conceptual studies of gamma ray diagnostics for DEMO control*, Fusion Eng. Des., vol. 136B, pp. 1494-1498, 2018 (online) https://doi.org/10.1016/j.fusengdes.2018.05.041.

[6] L. Giacomelli, *Contribution to advanced conceptual studies for neutron/gamma measurements on DEMO*, Final Report on Deliverable DC-4-T042-D002, Report IDM reference No. EFDA_D_2PG6ZD.

[7] E.V.D. van Loef et al., *Scintillation properties of LaCl3:Ce3+ crystals: Fast, efficient and high-energy-resolution scintillators*, Nucl. Instrum. Methods Phys. Res. A 486, 254 (2002).

[8] http://www.mcnp.ir/admin/imgs/1354175991.C715.PDF.

[9] M. Nocente et al., *Gamma-ray emission spectrum from thermonuclear fusion reactions without intrinsic broadening*, Nucl. Fusion 55 123009 (2015).

[10] M. Curuia, *Upgrade of the tangential gamma-ray spectrometer beam-line for JET DT experiments*, Fus. Eng. Des. 123, pp 749-753 (2017) https://doi.org/10.1016/j.fusengdes.2017.05.064.

[11] M. Nocente et al., *Conceptual design of the radial gamma ray spectrometers system for α particle and runaway electron measurements at ITER*, Nucl. Fusion 57 (2017) 076016 (12pp) https://doi.org/10.1088/1741-4326/aa6f7d.

[12] Y. Kim et al., *Determination of the deuterium-tritium branching ratio based on inertial confinement fusion implosions*, Phys. Review C 85 (2012) 061601(R).

[13] M. Cecconello et al., *DEMO diagnostic R&D: neutron/gamma diagnostics*, (VR) Final Report on Deliverable DC-4-T020-D001, Report IDM reference No. EFDA_D_2N5JVV.

[14] D.R. Tilley, H.R. Weller, C.M. Cheves, *Energy levels of light nuclei A = 16-17*, Nucl. Physics A 565 (1993) 1-184.

[15] J.M. Kebwaro et al., *Simulation of* $^{16}O(n, p)^{16}N$ *reaction rate and nitrogen-16 inventory in a high performance light water reactor with one pass core*, App. Rad. and Isotopes 94 (2014) 35-39.

[16] H.C. Martin, *Cross Sections for the* $O^{16}(n, p)N^{16}$ *Reaction from 12 to 18 MeV*, Phys. Review 93 3 (1954) 498.

[17] G.M. Hale, M.W. Paris, T. Kawano, ENDF/B-VIII.0 Los Alamos National Laboratory, Dec. 2017.

[18] G. Paic, I. Slasus, P. Tomas, $O^{16}(n, d)N^{15}{}_{gs}$ *and* $O^{16}(n, p)N^{16}$ *reactions at 14.4 MeV*, Phys. Letters 9 2 (1964) 147.

[19] G. Mazzone et al., *Divertor Cassette CAD update 2019*, WP-DIV-CAD-model-workshop_20190717.pptx, Report IDM reference No. EFDA_D_2MVK46.

[20] G. Mazzone et al., *Thermo-hydraulic assessment 2019*, DIV-1-T006-D006, Report IDM reference No. EFDA_D_2MVK46.

[21] ASME B36.19M-2018.pdf.

[22] Private communication with Dr. R. Luís and his presentation RaulLuis_Activation_Cooling_Water.pptx.

[23] V. G. Kiptily et al., *First Gamma-Ray Measurements of Fusion Alpha Particles in JET Trace Tritium Experiments*, Phys. Rev. Lett. 93, 115001 (2004).

[24] V.G. Kiptily, *On the core deuterium–tritium fuel ratio and temperature measurements in DEMO*, Nucl. Fusion 55 (2015) 023008 (7pp) doi:10.1088/0029-5515/55/2/023008.